International Journal of Wireless Information Networks (2022) 29:480–490
https://doi.org/10.1007/s10776-022-00577-4

Proximity Detection During Epidemics: Direct UWB TOA Versus Machine Learning Based RSSI

Zhuoran Su[1] · Kaveh Pahlavan[1] · Emmanuel Agu[2] · Haowen Wei[1,2]

Accepted: 21 September 2022 / Published online: 14 October 2022

Abstract
In this paper, we compare the direct TOA-based UWB technology with the RSSI-based BLE technology using machine learning algorithms for proximity detection during epidemics in terms of complexity of implementation, availability in existing smart phones, and precision of the results. We establish the theoretical limits on the precision and confidence of proximity estimation for both technologies using the Cramer Rao Lower Bound (CRLB) and validate the theoretical foundations using empirical data gathered in diverse practical operating scenarios. We perform our empirical experiments at eight distances in three flat environments and one non-flat environment encompassing both Line of Sight (LOS) and Obstructed-LOS (OLOS) situations. We also analyze the effects of various postures (eight angles) of the person carrying the sensor, and four on-body locations of the sensor. To estimate the range with BLE RSSI, we use 14 features for training the Gradient Boosted Machines (GBM) learning algorithm and we compare the precision of results with those obtained from memoryless UWB TOA ranging algorithm. We show that the memoryless UWB TOA algorithm achieves 93.60% confidence, slightly outperforming the 92.85% confidence of the BLE RSSI with more complex GBM machine learning (ML) algorithm and the need for substantial training. The training process for the RSSI-based BLE social distance measurements involved 3000 measurements to create a training dataset for each scenario and post-processing of data to extract 14 features of RSSI, and the ML classification algorithm consumed 200 s of computational time. The memoryless UWB ranging algorithm achieves more robust results without any need for training in less than 0.5 s of computation time.

✉ Zhuoran Su
zsu2@wpi.edu

Kaveh Pahlavan
kaveh@wpi.edu

Emmanuel Agu
emmanuel@wpi.edu

Haowen Wei
hwei@wpi.edu

[1] Electrical and Computer Engineering, Worcester Polytechnic Institute, 100 Institute Road, Worcester, MA 01609, USA

[2] Computer Science, Worcester Polytechnic Institute, 100 Institute Road, Worcester, MA 01609, USA

Graphical Abstract

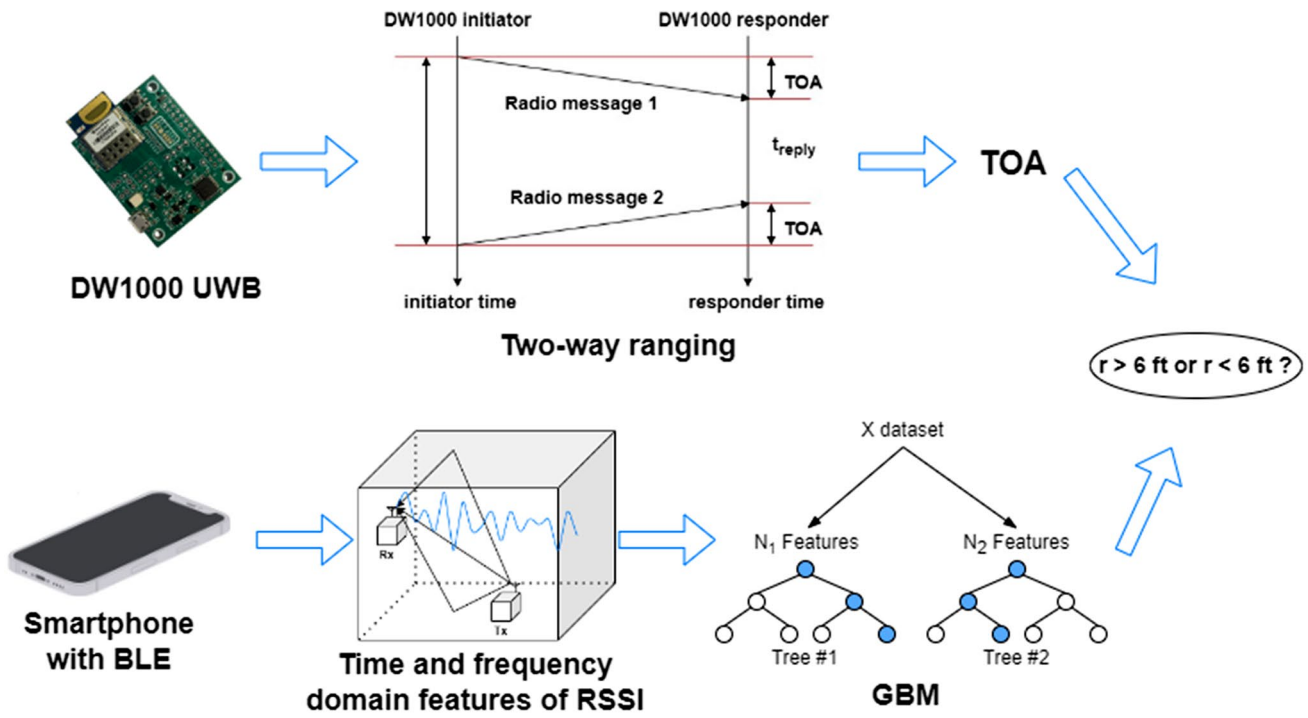

Keywords COVID-19 · Proximity detection · RSSI features · Classical estimation theory · BLE · UWB

1 Introduction

The Covid-19 epidemic revealed the importance of research in opportunistic social distance estimation during the epidemics using the Received Signal Strength Indicator (RSSI) of Bluetooth Low Energy (BLE) wireless technology, which are commonly available in smartphones [1–3]. Due to the effects of multipath and shadow fading on RSSI-based ranging, direct estimation of distance using RSSI is unreliable as it is compared with time-of-arrival (TOA) based positioning [gezici, pah19]. However, due to availability of BLE in smartphones a new trend of research to improve the performance of RSSI-based ranging with machine learning algorithms [4] and hybrid positioning approaches that integrate additional information from various mechanical sensors (e.g. accelerometer and gyroscope) that are built into many smartphones [5] has attracted considerable attention in recent literature. Ultra-Wideband (UWB), an alternative emerging popular wireless technology, offers a more precise Time-of-Arrival (TOA) range without requiring complex ML algorithms that need extensive training and large amounts of labeled training data. Inexpensive UWB devices are already available in the market and the existing 5G cellular networks support UWB positioning. What is lacking in the literature is the comparison of these improved RSSI-based ranging with the UWB ranging. Time of arrival (TOA) based ranging with the ultrawide (UWB) signals [6, 7] has emerged as an alternative to unreliable, opportunistic RSSI-based BLE ranging. The reuse of existing popular devices, which already have the circuitry required for both UWB and BLE RSSI, could facilitate rapid, wide-scale deployment and curb epidemics quickly. With the recent emergence of low cost UWB devices [8] and the 3GPP recommendation of TOA base ranging for 5G and beyond [9–12], TOA-based UWB social distance estimation has become a viable alternative to BLE RSSI. In comparison to ML algorithms that require large amounts of labeled training data and an extensive training process, the UWB approach utilizes real-time algorithms that do not require training or memory, while still achieving high precision ranging and confidence on proximity estimates.

The objective of this study is to establish a theoretical foundation for comparing the precision and confidence in the protocols for measuring social distance using BLE RSSI and UWB TOA devices, and to validate this theoretical basis using empirical data gathered in practical scenarios. Using the Cramer Rao Lower Bound (CRLB) of RSSI and TOA ranging [6, 7], the theoretical foundations enable derivation and analyses of precision and confidence of estimated social distance. We expand the derivation of confidence for

RSSI-based ranging previously presented in [4] to include TOA-based ranging, which we then validate using empirical data gathered in multiple practical scenarios using BLE and DecaWave UWB devices. We perform empirical experiments at eight distances in three flat environments and one non-flat environment encompassing both Line of Sight (LOS) and Obstructed-LOS (OLOS) situations. We also analyze the effects of various postures (eight angles) of the person carrying the sensor, and four on-body locations of the sensor. To estimate range using BLE RSSI, 14 RSSI features were classified using the Gradient Boosted Machines (GBM) ML algorithm. The empirical results for TOA ranging using memoryless algorithms are derived from data gathered using inexpensive, off-the shelf UWB DecaWave chipsets. To the best of our knowledge, our analysis is the first to systematically compare BLE RSSI and UWB TOA for social distance estimation using rigorous theoretical foundations.

The rest of this paper is as follows. In part II, we introduce the data gathering scenarios we investigated and provide details of our dataset. In part III, we present the relevant theoretical foundations including the calculation of CRLB, as well as the derivation of confidence of proximity detection and corresponding bounds. In part IV, we present experiments to validate the theoretical foundations presented in part II, for the comparative performance evaluation of proximity detection using BLE RSSI and UWB TOA.

2 The Promixity Datasets and Measurements Scenarios

This study builds on our previous study reported in [4], in which we analyzed the existing MITRE Range Angle Structured (MRAS) dataset [13] provided by the Private Automated Contact Tracing (PACT) consortium. The MRAS dataset contains RSSI measurements gathered using BLE devices in various testing scenarios at different distances in flat Line-Of-Sight (LOS) situations. Since the existing MRAS dataset only includes BLE RSSI data, to facilitate a comparison with UWB, we had to conduct experiments to gather UWB TOA measurements. Specifically, in this study, we collected our own dataset to enable comparative performance evaluation of range estimation using BLE RSSI and TOA gathered using DecaWave 1000 UWB technologies. To ensure a fair comparison, we collected data from both device types in the exact same locations, environments, and scenarios. Similar to the PACT dataset, our dataset scenarios were rich, including various room sizes and on-body positions in which the measurement device was carried/held by the owner of the test device. We also expanded on prior measurement scenarios, and included more diversified situations consisting of LOS as well as Non-Line-Of-Sight (NLOS), and non-flat staircase scenarios. Figure 1a and b provide an overview of our measurement scenarios. In Fig. 1a, transmitter-receiver distances ranging between 3 and 12 ft were selected as these have been found to be the most challenging distances when detecting a social distance of 6 feet is the objective (as recommended for Covid-19). Beyond 8 feet, the intervals between the transmitter and receiver were increased in order to generate more significant RSSI differences. Figure 1b shows the four on-body locations in which subjects carried their smartphones. In this study, we also considered two postures, standing and sitting. The transmitter is always positioned at the 0 ft location, while the receiver moves at increments to enable measurements at distances ranging from 3 to 12 ft. In order to simulate the effects of shadow fading, at each stationary location, while holding the device, the tester turned 45° clockwise with the same posture. Since we defined the transmitter and receiver being face-to-face as 0°, RSSI and TOA were collected at eight angles at increments of 45°. At each test location shown in Fig. 1a, data was gathered for 30–40 s, which typically contained 300–400 RSSI samples or 64 TOA samples, which were stored in our dataset as depicted by Eq. (1).

$$\begin{cases} p(k) = \text{RSSI}(t)|_{t=kT_p}; & k = 1, \ldots, N \\ \tau(k) = \text{TOA}(t)|_{t=kT_\tau}; & k = 1, ...M \end{cases} \tag{1}$$

where $p(k)$ and $\tau(k)$ are the k-th sample in the RSSI and TOA time series collected, respectively. N and M are the numbers of samples collected. Since N has values in the range 300–400 and M is 64 in this study, we selected T_p and T_τ, the time intervals of RSSI and TOA samples to ensure that data was gathered in approximately the same 30–40 s interval for both the BLE and UWB devices. Table 1 shows details of our environment settings. We collected our data in 4 environments: a large room (a large laboratory), medium room (a meeting room), hallway (the corridor), and stairway (an indoor staircase). In each environment, the transmitter (an iPhone 7) and receiver (an iPhone 12) were separated by a wall for the NLOS scenario. For the LOS scenario, the transmitter and receiver were positioned in the center of an environment with no obstacle between them. While collecting data, the two testers were required to hold the phone in specific on-body locations (see the fourth row in Table 1). Their posture was either sitting or standing at a given location.

We observed a variation of up to 25 dB RSSI in one scenario. In order to reduce the significant effects of fading on the amplitude of the received signal from which we calculated the RSSI, our study for RSSI included classical and Machine Learning (ML) algorithms. Variations of amplitude do not have drastic effects on TOA measurements and the results of TOA measurement can be utilized directly for range estimation. The RSSI measurements

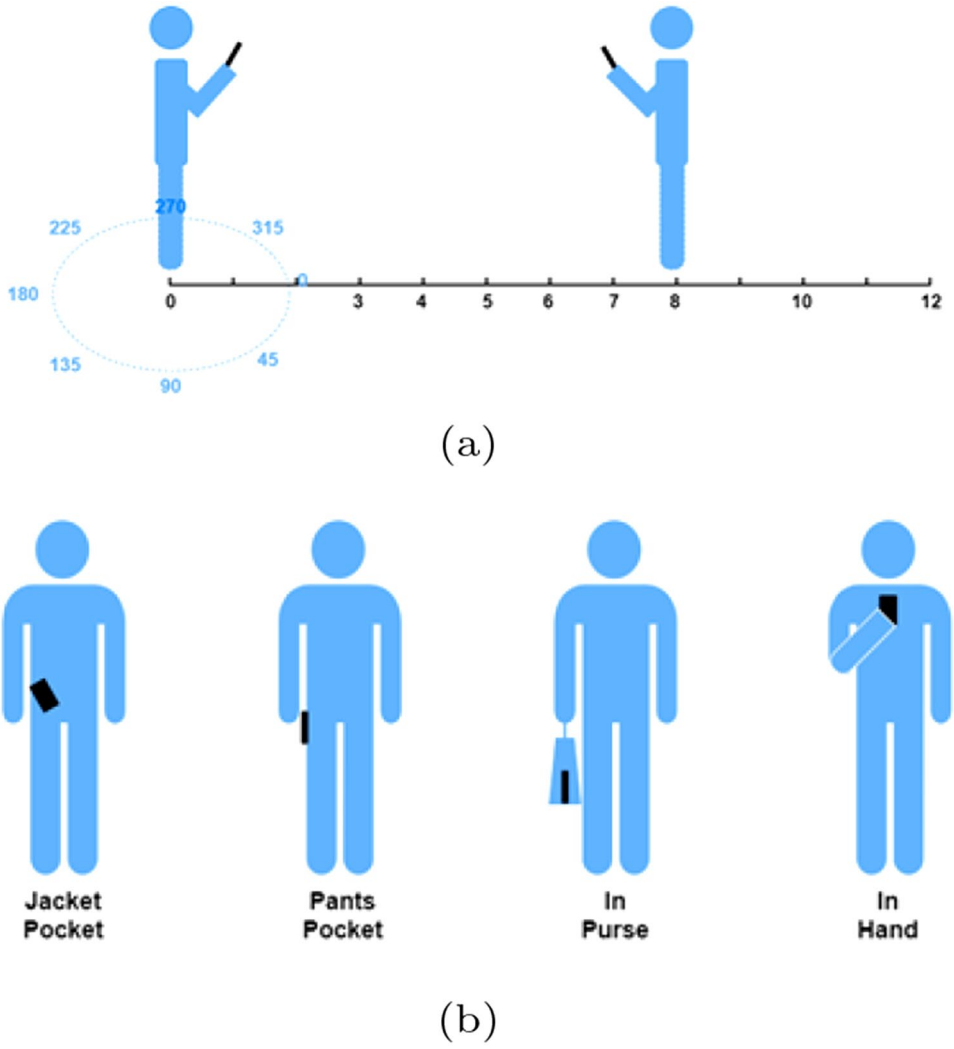

Fig. 1 Measurement scenarios used to gather our dataset, **a** eight distances (ft) and eight angles (degrees) for the dataset. **b** four on-body locations for the BLE and UWB devices

Table 1 Measurement scenarios used to gather data for our dataset

Scenarios	Settings
Description of the areas	Medium room, Large room hallway, Stairway
Multipath scenario	LOS, NLOS
Type of device	iPhone 7, iPhone 12
Device location (on-body)	In hand, In purse, Pants pocket, Jacket Pocket
Tester's posture	Standing, sitting

in each location, defined by Eq. (1), are post-processed before feeding them in different ways into classical and ML algorithms. For classical estimation algorithms, we utilized the average of RSSI and TOA measurements gathered in each location as defined by Eq. (2):

$$\begin{cases} P_r = \frac{1}{N}\sum_{k=1}^{N} p(k) \\ r = \frac{1}{M}\sum_{k=1}^{M} \tau(k) \end{cases} \quad (2)$$

This post processing of data associates a single average RSSI measurement, Pr with a single average TOA measurement, τ_r for each location. For ML techniques, the 300–400 RSSI measurements in each location were grouped in overlapping sets of RSSI measurement vectors of length L, whose elements are defined by Eq. (3).

$$S(n, L) = \{P(k+n);\ k = 0, 1, ..L-1\};\ n = 1, ...N-L \quad (3)$$

This processing associates an $N - L$ set of L dimensional vectors to each location. Similar to [4], our performance criterion is the confidence of the correctness of the decision by the algorithm on whether the inter-subject distance is less than vs. over the social distance of 6 ft. Evaluation

was done using BLE RSSI (smartphone) or UWB TOA (DW1000 receiver) measurements gathered at the same location, respectively.

3 Theoretical Foundations for Data Analysis

In this section, we introduce theoretical foundations derived from classical estimation theory. We relate the variance of observations (P_r and τ) with the CRLB and then derive equations for the standard deviation of distance estimates as a function of the ground truth. With the assumption that the noise is a zero-mean Gaussian distribution, we are able to derive the upper bound for the performance of the proximity detection problem using the complementary error function (erfc). For RSSI-based ranging, we employ a linear regressive model of the average received powers in the zero mean Gaussian distributed shadow fading, X(σ), with a fixed variance of σ, enabling us to formulate the classical approach based on observation of the average RSSI [4]:

$$O: P_r = P_0 - 10\alpha \log(r) + X(\sigma), \tag{4a}$$

Our objective is to estimate the range r. To estimate range using the TOA, we formulate the problem based on direct observation of range by multiplying the average TOA [14]:

$$O: \quad r = c \times \left[\tau + \eta(\sigma_\tau)\right] = r + c \times \eta(\sigma_\tau) = r + \eta(\sigma_r), \tag{4b}$$

where c is the speed of light, and $\eta(\sigma_r)$ is the variance of TOA measurement noise determined from the CRLB of the TOA measurement. Equation (4b) is a function of pulse shape, bandwidth, W, and the received Signal to Noise Ratio (SNR), which provides a lower bound on the variation of the estimation [15]:

$$\sigma_1(r) = \sqrt{\text{CRLB}} \geq \frac{\ln 10}{\sqrt{N}10} \frac{\sigma}{\alpha} r \tag{4c}$$

Using classical estimation theory, formulating the observation of a function of a noise parameter yields two functions: (1) the traditional RSSI linear regression model [4], and (2) the simple TOA [14] model for distance measurement (Eq. 4d).

$$\sigma_r = c \times \sqrt{\text{CRLB}} \geq \frac{c}{2\pi\sqrt{2 \times \text{SNR} \times W \times T_M \times {f_0}^2}} \tag{4d}$$

Compared with BLE RSSI, the model for UWB TOA requires more parameters due to the difference in ranging algorithms utilized. Leveraging classical estimation theory, we relate the variance of distance estimates with the variance of RSSI and TOA measurements by introducing the CRLB. In addition, we show that the theoretical analyses works not only for BLE but also for UWB, even though they utilize completely different algorithms to estimate distance.

3.1 Maximum Likelihood Range Estimation and CRLB for Ranging Error

In classical estimation theory, the optimal maximum likelihood estimate of the range, is the inverse of $g(r)$, the observation function Eq. (5a):

$$\hat{r} = g^{-1}(O). \tag{5a}$$

Therefore, the optimal Maximum Likelihood Estimates (MLE) of range from average RSSI and TOA measurements are given by Eq. (5b):

$$\begin{cases} \hat{r}_{\text{RSSI}} = {g_{\text{RSSI}}}^{-1}(P_r) = 10^{-\frac{P_r - P_0}{10\alpha}} \\ \hat{r}_{\text{TOA}} = {g_{\text{TOA}}}^{-1}(r) = r = c \times \tau \end{cases} \tag{5b}$$

The variance of this estimation is the CRLB, which is the inverse of the Fisher Information Matrix (FIM) of the dataset Eq. (6a), calculated in [14]:

$$\sigma^2(r) = \text{CRLB} \geq \frac{{\sigma_M}^2}{\left[g'(r)\right]^2}, \tag{6a}$$

where $\sigma(r)$ is the variance of ranging error, $g(r)$ is defined by Eq. (5b), and σ_M is the standard deviation of measurement noise. For the RSSI measurements, the standard deviation of shadow fading, and for TOA, was defined by Eq. (4c). With the two proposed models Eqs. (4c) and (4d), and the CRLB given in Eq. (6a), the standard deviation of distance estimates is given by Eq. (6b).

$$\begin{cases} \sigma_{RSSI}(r) = \sqrt{\text{CRLB}} \geq \frac{\ln 10}{\sqrt{N}10} \frac{\sigma}{\alpha} r \\ \sigma_{TOA}(r) = c \times \sqrt{\text{CRLB}} \geq \frac{c}{\sqrt{N}2\pi\sqrt{2\text{SNR}(r) W T_M {f_0}^2}}, \end{cases} \tag{6b}$$

where N is the number of samples (300–400 for RSSI and 64 for TOA), and where SNR(0) is the Signal to Noise Ratio at a reference distance.

3.2 Derivation of Bounds on Confidence and Validation with Empirical Measurements

When we estimate a range, r, from noisy RSSI or TOA measurements, the characteristics of the noise can be used to calculate the confidence on estimates. Our definition of confidence in this study is the probability of correct prediction that an estimated distance is less or larger than 6 ft when the ground truth is also less or larger than 6 ft (expressed in Eq. 7a).

$$\gamma(r) = \Pr\left\{\left[\hat{r} \le 6/r \le 6\right] OR \left[\hat{r} > 6/r > 6\right]\right\} \tag{7a}$$

Confidence is a function of distance and reflects the degree of assurance of proper detection by the algorithm. For RSSI-based ranging, modeled by Eq. (4a), and its maximum likelihood estimate given by Eq. (5b), the confidence on ranging at a given distance r is given by Eq. (7b).

$$\begin{aligned}\gamma(r) &= \Pr\left\{\left[\hat{r} \le 6/r \le 6\right] OR \left[\hat{r} > 6/r > 6\right]\right\} \\ &= \Pr\left\{\left[\hat{r} \le 6/P_r \le P_6\right] OR \left[\hat{r} > 6/P_r > P_6\right]\right\} \\ &= 1 - \frac{1}{2}\mathrm{erfc}\left(\frac{|P_6 - P_r|}{\sqrt{2}\sigma}\right),\end{aligned} \tag{7b}$$

where P_6 is the expected RSSI at a 6 ft distance calculated using Eq. (4a). In this study, we apply the Least Square (LS) algorithm to the collected RSSI data and calculate the empirical parameter (P_0, α, σ) in Eq. (4a) before estimating P_6. In our RSSI database, there are 300–400 measurements at each location, and we calculate confidence for each of these measurements, which are then averaged over the entire set (dashed blue line in Fig. 4). For empirical ranging with TOA measurements, we utilize Eq. (5b) directly multiplying the measured TOA by the speed of light and then check whether the estimated value is to the right side of 6-ft. These range estimates are averaged over the 64 TOA measurements to determine the empirical value of the confidence at each location in the dataset (dashed red line in Fig. 4).

We are also able to calculate confidence bounds on the range estimate as a function of distance from the calculation of the CRLB given by Eq. (6b). The CRLB provides the estimate of the variance of a parameter from the function relating the parameter to the measurement or observation. In [4], the Distance Measurement Error (DME) of BLE RSSI is given as:

$$\hat{r} - r = \eta[\sigma(r)] \tag{8a}$$

$\sigma(r)$ is the standard deviation of $\hat{r}$ given in Eq. (6b). $\eta_[\sigma(r)]$ is a zero-mean Gaussian distribution. The confidence bound for BLE RSSI is (Eq. 8b):

$$\begin{aligned}\gamma(r) &= \Pr\left\{\left[\hat{r} \le 6/r \le 6\right] \cap \left[\hat{r} > 6/r > 6\right]\right\} \\ &= 1 - \frac{1}{2}\mathrm{erfc}\left(\frac{|6 - r|}{\sqrt{2}\sigma(r)}\right),\end{aligned} \tag{8b}$$

where $\gamma(r)$ is the probability of making correct proximity detection decisions. In Eq. (7a), $\gamma(r)$ is the actual probability calculated from real data. However, in Eq. (8b), $\gamma(r)$ is the theoretical upper bound for a given distance r.

4 Comparison of Ranging with BLE and UWB Signals

In this section, we will first introduce the accuracy of ranging and its theoretical bounds since the confidence of proximity detection is highly related to it. As shown is Sect. 1, the theoretical foundation of this paper consists of two parts: (1) the bound of DME which is calculated from Eq. (6b), and (2) the bound on proximity detection confidence, which is calculated from Eq. (8b). In this section, we present the simulation results of the theoretical bounds as well as the empirical results obtained from BLE RSSI and UWB TOA data. Figure 2 shows the overall structure of the performance evaluation in this section. The UWB TOA is obtained using a two-way ranging approach provided by Decawave. Both a classical regression model and an ML algorithm (GBM), are evaluated on BLE RSSI data. We utilize the confidence defined in Sect. 3.2 as the criterion for performance evaluation. The suggested 6 ft social distance is the decision threshold. If the ground truth $r < 6$ ft, the confidence is the probability $P\{\hat{r} < 6\,\text{ft} | r < 6\,\text{ft}\}$. Similarly, if the ground truth $r > 6$ ft, the confidence is the probability $P\{\hat{r} > 6\,\text{ft} | r > 6\,\text{ft}\}$.

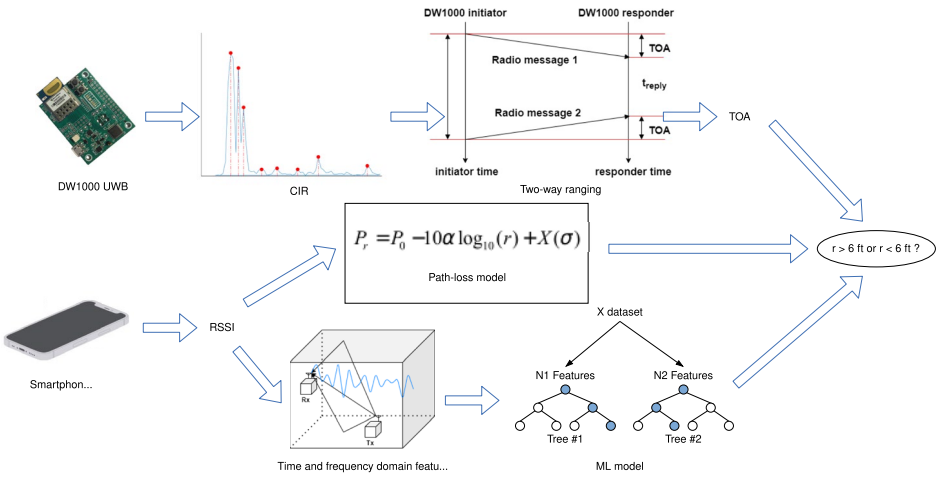

Fig. 2 Workflow for performance evaluation: UWB TOA was gathered using DW1000, classical path-loss model utilized for BLE RSSI, and GBM for extracted RSSI features

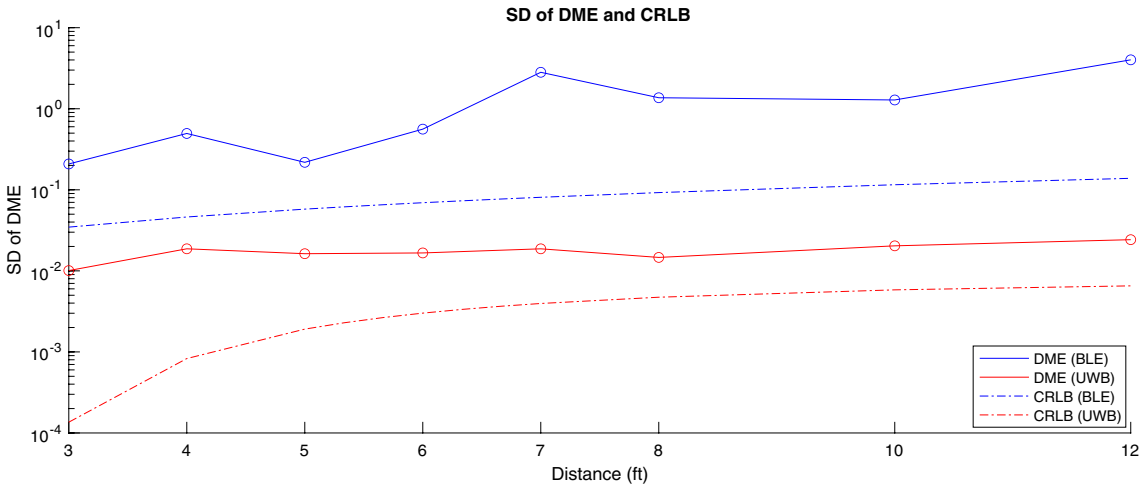

Fig. 3 CRLB (dashed lines) versus the standard deviation of DME (solid lines)

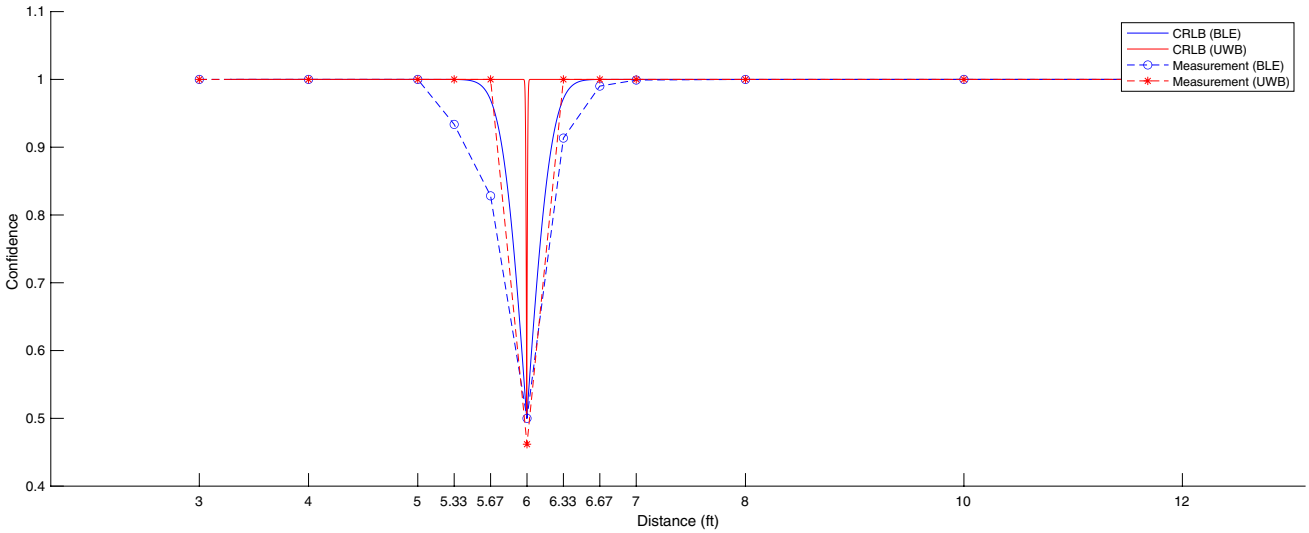

Fig. 4 Bounds on confidence on estimate as a function of distance (solid lines) versus performance of collected dataset (dashed lines)

We begin by calculating DME for both RSSI and TOA. Then we present the bounds on confidence of RSSI and TOA based ranging, respectively. We also evaluate the performance of BLE and UWB in various environments, which is presented in Sect. 4.2.

For BLE RSSI, we first calculate the parameters of the path loss model in Eq. (4a) by applying the Least Square Estimate (LSE) algorithm. Then, to compute the bound or confidence, we substitute the parameter values calculated into Eq. (8b). As shown in Fig. 2, we use the GBM ML algorithm to decide whether the distance between two devices is within the 6 ft range. To train a GBM, we extracted 14 features, including frequency-domain and time-domain features. The training set and test set were 80% and 20%, respectively. For UWB TOA, the theoretical confidence bound is also computed using Eq. (8b). The empirical confidence at a certain distance is simply calculated as the ratio of the count of correct decisions and the number of total samples. Then we calculated the standard deviation of TOA measurement and plugged the value into Eq. (6b) to calculate the CRLB of TOA. For all scenarios described in Table 1, the parameters for RSSI regression model (Eq. 4a) is $P_0 = -46.80$dBm, $\alpha = 2.07$ and $\sigma = 3.41$ dB. And the CRLB parameters for TOA (Eq. 4c) are preset for Deca 1000 transceivers. They are $f_0 = 3993.6$ MHz, $M = 499.4$ MHz, and $T_M = 26$ ms. We use the first meter SNR as the reference and assume the SNR is inversely proportional to the squared distance.

4.1 Results of Theoretical Foundations Analysis

Since we have already calculated the required parameters for CRLB, we first compare the lower bound of the standard deviation of DME. As shown in Fig. 3, the two dashed lines are the CLRB obtained by substituting the parameters into Eq. (6b). At all distances, the TOA has a much lower CRLB (the lower dashed line) compared to the CRLB of RSSI (the upper dashed line), which means the UWB TOA is more accurate than BLE RSSI. Next, we calculate the actual SD of DME by calculating Fig. 4 the standard deviation of the difference between distance estimates and the ground truth shown in Fig. 1a) The two solid lines in Fig. 3 are the observed results. For both RSSI and TOA estimates, the SD of DME is always above the corresponding CRLB. Figure 3 shows that Eq. (6b) holds for the estimate generated using the TOA-based, two-way ranging algorithm as well as the GBM-based RSSI estimate.

Using the correct CRLB, we can then analyze the main criterion in this study, the confidence of proximity detection. The theoretical confidence bounds for TOA and RSSI are both calculated using Eq. (6b). For RSSI, we input the 14 features into GBM, and it outputs whether the estimated distance is in the 6 ft range. For TOA, we multiply the speed of light by the estimated time and then compare the result with 6 ft to decide whether it is within the 6 ft range. Figure 4 shows the proposed confidence bound (solid lines) and the empirical confidence calculated from the collected dataset (dashed lines). The V-shape bounds show the best performance of these two approaches on the test dataset. The solid red line is the bound of UWB TOA estimates, and the solid blue line is the bound of BLE RSSI estimates. Both approaches show approximately 100% confidence when the ground truth is far from the threshold ($r > 7$ ft and $r < 5$ ft). Theoretically, UWB TOA can achieve much better performance around 6 ft because it has a narrow distance interval with low confidence. To achieve a more precise comparison in low-performance areas, we added two more locations between 5 and 6 ft and two more locations between 6 and 7 ft. For the distances far from the threshold ($r > 7$ ft and $r < 5$ ft), the two-way ranging and GBM have almost the same confidence as the theoretical bounds. For the low confidence range ($5 < r > 7$ ft), UWB TOA shows much higher confidence than BLE RSSI. At exactly 6 ft, both algorithms have the lowest confidence. Our empirical result shows that the confidence at all distances is consistently less than or equal to the upper bound calculated from Eq. (8b), and that UWB TOA outperforms BLE RSSI when the distance is close to 6 ft.

4.2 Effect of Measurement Scenario

In this section, we present the results of BLE RSSI and UWB TOA in various environments and scenarios described in Table 1. We use the average confidence at eight locations and eight angles shown in Fig. 1a as the performance criteria. As shown in Fig. 4, the most significant confidence difference is observed between 5 and 7 ft. Since the eight selected locations are distributed between 3 and 12 ft, the difference between the average confidences of BLE RSSI and UWB TOA is not very significant (less than 5%). While comparing the performance in different environments, the user's posture and on-body location they carried the device were always "standing" and "in hand", respectively.

We began our performance evaluation as well as analysis of the effect of parameters by comparing the confidence calculated from GBM predictions on BLE RSSI and the confidence from two-way ranging on UWB TOA in different environments. Table 2 shows our results in eight environment settings. The best result of BLE RSSI is obtained in the large room with LOS scenario (94.38 %) and the worst result is obtained in the staircase with an LOS scenario (91.18%). For BLE RSSI, the confidence difference is up to 2.7% considering LOS and NLOS and 3.2% for different room sizes. The average confidence of BLE RSSI is 92.84%. The best and worst results of TOA are 94.63% and 87.5% in the medium room and staircase respectively. The confidence difference of TOA is 7.08% and 6.49% for varied room size and multipath scenarios, respectively. UWB TOA has 0.5% more confidence than BLE RSSI. Table 3 shows confidence for various postures and on-body locations described in Fig. 1b. First, we keep the user behavior fixed (both testers hold their phones in hand) and discuss the effect of user postures. Tester1 is the person who holds the transmitter and Tester2 holds the receiver. For the BLE RSSI approach, confidence is 2.43% higher if Tester1 was standing, compared to results when Tester1 was sitting. The best result is obtained when both testers are sitting, which is 94.34%. and

Table 2 Effect of environment on confidence

Environment		Confidence (%)	Confidence (%)
Room size	Multipath scenario	BLE RSSI (GBM)	UWB TOA
Medium room	LOS	94.02	94.19
	NLOS	93.30	94.63
Large room	LOS	94.38	94.43
	NLOS	93.04	94.58
Hallway	LOS	92.18	93.85
	NLOS	91.79	94.34
Stairway	LOS	91.18	94.04
	NLOS	93.68	87.55

Table 3 Effect of user behavior (Tester's posture and location of phone) on confidence

Posture		Device on-body location		Confidence (%)	Confidence (%)
Tester1	Tester2	Tester1	Tester2	BLE RSSI (GBM)	UWB TOA
Sitting	Standing	In Hand	In Hand	93.39	93.55
			Jacket Pocket	94.28	94.34
			Pants Pocket	90.28	93.26
			In Purse	93.99	95.12
	Sitting	In Hand	In Hand	94.34	93.75
Standing	Standing	In Hand	In Hand	92.49	93.07
	Sitting	In Hand	In Hand	90.39	93.31

the worst result of 90.3% is obtained when Tester1 is sitting and Tester2 is sitting. Thus, we conclude that different postures can cause up to 3.95% confidence. However, different postures do not cause huge variations in the result of UWB. As shown in the last column in Table 3, the maximum confidence difference for various postures and on-body locations is 0.68%. To compare the effect of on-body location of the device, we kept the postures fixed (sitting and standing). The confidence differences are 4% and 1.86% for BLE RSSI and UWB TOA, respectively. The change of on-body location affected BLE RSSI more, while the change in the multipath environment affected UWB TOA more.

In this section, we presented an empirical comparative performance evaluation of proximity detection for the social distance using the RSSI of the BLE and TOA of the DecaWave UWB devices. To evaluate the performance, we used the confidence on whether a tester is within the social distance (6 feet) as the primary criterion. We provided a novel theoretical foundation with classical estimation theory using the CRLB to develop bounds for the confidence. Then we compared the performance of UWB TOA obtained by a two-way ranging algorithm with a BLE RSSI-based machine learning algorithm against these bounds. We found that for both UWB TOA and BLE RSSI, the empirical result is almost the same as the theoretical bound if the ground truth is far from the boundary (6 feet). However, both the theoretical bound and the empirical result have the worst performance when approaching the boundary. The theoretical foundations show that the average confidence of UWB TOA estimation for the distance between 3 and 12 feet is 96.98%, which is 1.58% better than utilizing BLE RSSI. To validate the theoretical bounds and evaluate the confidence provided by BLE RSSI and UWB TOA, we collected a novel dataset in fifteen scenarios in order to obtain a fair comparative analysis. For both LOS and OLOS situations, we conducted experiments in three flat environments (medium and large rooms, and corridor) and an environment where the transmitter and receiver are placed at different heights (stairway). The 7 other scenarios involved varying the tester's postures (sitting and standing) and the places where one tester carried the receiver (in hand, jacket pocket, pants pocket, and purse). A machine learning model based on the GBM algorithm was trained using BLE RSSI data for each scenario to estimate the confidence. For the UWB, the TOA is obtained directly using the Decawave two-way ranging algorithm. UWB TOA outperforms BLE RSSI in almost all environments except the staircase environments with a NLOS situation and both testers were sitting. For BLE RSSI, different postures caused up to 3.95% confidence difference. However, the maximum confidence difference obtained by UWB TOA was only 0.68%. On average, the confidence of UWB TOA was 0.75% better than that of BLE RSSI, which means that the proposed theoretical bound is consistent with the empirical result. Theoretically, the proposed theoretical foundation gives us a relation between the traditional CRLB and the confidence of proximity detection and a bound for confidence as a function of distance. Practically, the theoretical foundation provides an approach to analyze whether a technique is suitable for solving the proximity detection problem.

5 Conclusion

The availability of TOA-based UWB positioning in emerging, inexpensive IoT devices and the 5G cellular networks has created an alternative to RSSI-based BLE positioning for proximity detection for social distancing. The UWB solution operates in real-time without a need for training a complex ML algorithm for RSSI-based ranging. In this paper, we presented an empirical comparative performance evaluation of proximity detection for social distance using BLE RSSI features classified offline using a complex GBM ML algorithm and TOA data from the DecaWave UWB devices using a simple real-time, memoryless algorithm embedded on the device. To evaluate the performance, we used the confidence on whether a tester is within the social distance (6 feet) as the primary criterion. We provided a novel theoretical foundation with classical estimation theory using the CRLB to develop bounds for the confidence. Then we compared the performance of UWB TOA obtained using a two-way ranging algorithm with BLE RSSI-based approach using a GBM

ML algorithm against these bounds. We demonstrated that even without any training, the UWB TOA can outperform BLE RSSI using the GBM ML algorithm. We expect that the next generation of social distance monitoring systems transfer from RSSI based to TOA based technologies.

Acknowledgements The authors would like to acknowledge contributions of Dr. Nader Moayeri of the National Institute of Standard and Technology for fruitful discussions on development of thoughts resulting in this research and his productive comments on the reference [4] that laid the foundation of this study. This work was supported in part by the Defense Advanced Research Projects Agency (DARPA) Warfighter Analytics using Smartphones for Health (WASH) Program under Agreement FA8750-18-2-0077.

References

1. A. Ghose, C. Bhaumik, and T. Chakravarty, Blueeye: A system for proximity detection using bluetooth on mobile phones. In: Proceedings of the 2013 ACM Conference on Pervasive and Ubiquitous Computing Adjunct Publication, pp. 1135–1142, 2013.
2. S. Liu, Y. Jiang, and A. Striegel, Face-to-face proximity estimationusing bluetooth on smartphones, *IEEE Transactions on Mobile Computing*, Vol. 13, No. 4, pp. 811–823, 2013.
3. S. Shankar, R. Kanaparti, A. Chopra, R. Sukumaran, P. Patwa, M. Kang, A. Singh, K. P. McPherson, and R. Raskar, Proximity sensing: Modeling and understanding noisy rssi-ble signals and other mobile sensor data for digital contact tracing. arXiv preprint arXiv:2009.04991, 2020.
4. Z. Su, K. Pahlavan, and E. Agu, Performance evaluation of covid-19 proximity detection using bluetooth le signal, *IEEE Access*, Vol. 9, pp. 38891–38906, 2021.
5. O. Semenov, E. Agu, K. Pahlavan, and Z. Su, Covid-19 social distance proximity estimation using machine learning analyses of smartphone sensor data, *IEEE Sensors Journal*. https://doi.org/10.1109/JSEN.2022.3162605, 2022.
6. S. Gezici, and H. V. Poor, Position estimation via ultra-wide-band signals, *Proceedings of the IEEE*, Vol. 97, No. 2, pp. 386–403, 2009.
7. A. Hatami, and K. Pahlavan, Performance comparison of rss and toa indoor geolocation based on uwb measurement of channel characteristics. In: 2006 IEEE 17th International Symposium on Personal, Indoor and Mobile Radio Communications, pp. 1–6, 2006. IEEE.
8. DW1000, 3.5 - 6.5 GHz Ultra-Wideband (UWB) Transceiver IC with 1 Antenna Port, 2022. https://www.decawave.com/product/dw1000-radio-ic/.
9. S. Dwivedi, R. Shreevastav, F. Munier, J. Nygren, I. Siomina, Y. Lyazidi, D. Shrestha, G. Lindmark, P. Ernström, and E. Stare, et al., Positioning in 5g networks, *IEEE Communications Magazine*, Vol. 59, No. 11, pp. 38–44, 2021.
10. A. Dammann, R. Raulefs, and S. Zhang, On prospects of positioning in 5g. In: 2015 IEEE International Conference on Communication Workshop (ICCW), pp. 1207–1213, 2015. IEEE.
11. R. Keating, M. Säily, J. Hulkkonen, and J. Karjalainen, Overview of positioning in 5g new radio. In: 2019 16th International Symposium on Wireless Communication Systems (ISWCS), pp. 320–324, 2019. IEEE.
12. F. Wen, J. Kulmer, K. Witrisal, and H. Wymeersch, 5g positioning and mapping with diffuse multipath, *IEEE Transactions on Wireless Communications*, Vol. 20, No. 2, pp. 1164–1174, 2020.
13. Structured Contact Tracing Protocol, Boston, MA, 2020. https://mitll.github.io/PACT/.
14. K. Pahlavan, *Indoor Geolocation Science and Technology*, pp. 104–109. River Publishers, Denmark, 2019.
15. K. Pahlavan, J. Ying, Z. Li, E. Solovey, J. P. Loftus, and Z. Dong, Rf cloud for cyberspace intelligence, *IEEE Access*, Vol. 8, pp. 89976–89987, 2020.

Zhuoran Su (Student Member, IEEE) received the B.S. degree in communication engineering from Beijing Jiaotong University (BJTU), Beijing, China, in 2017, and the M.S. degree in electrical and computer engineering (ECE) from the Worcester Polytechnic Institute (WPI), Worcester, USA, in 2020, where he is currently continuing his research and pursuing the Ph.D. in ECE at WPI. His main fields of research interest are in indoor channel modeling, indoor localization, human motion detection and gesture detection using RF signals, and deep learning using RF signals.

Kaveh Pahlavan (Life Fellow, IEEE) was a Westin Hadden Professor of electrical and computer engineering with the Worcester Polytechnic Institute (WPI), Worcester, MA, from 1993 to 1996. He is currently a professor of electrical and computer engineering, a Professor of computer science, the Director of the Center for Wireless Information Network Studies, WPI, and the Chief Technical Advisor of Skyhook Wireless, Boston, MA. He has authored the books Wireless Information Networks (John Wiley and Sons, 1995), Wireless Information Networks (John Wiley and Sons, Second Edition, 2005) (with Allen Levesque), Principles of Wireless Networks—A Unified Approach (Prentice Hall, 2002) (with P. Krishnamurthy), and Networking Fundamentals: Wide, Local, and Personal Communications (Wiley, 2009) (with P. Krishnamurthy). His current area of research is opportunistic localization for body area networks and robotics applications. He received the Nokia Fellowship, in 1999, and the first Fulbright-Nokia Scholar with the University of Oulu, Finland, in 2000.

Emmanuel Agu (Member, IEEE) received the Ph.D. degree in electrical and computer engineering from the University of Massachusetts Amherst, Amherst, MA, USA, in 2001. He is a Professor with the Computer Science Department, Worcester Polytechnic Institute, Worcester, MA. He has been involved in research in the mobile and ubiquitous computing. He is currently working on mobile health projects to assist patients with diabetes, obesity, depression, wounds, TBI, and infectious diseases.

Haowen Wei (Student Member, IEEE) is currently pursuing his Electrical and Computer Engineering and Computer Science B.S. degree with the Worcester Polytechnic Institute. He works at the Center for Wireless Information Network Communication Laboratory (CWINS) and Advanced Human-Computer-Interaction Laboratory and researches the real-time touch-free gesture motion detection system. His main research interests are the advanced Brain-Computer Interface (BCI) paradigm and its corresponding applications.